 DOI: 10.3217/978-3-85125-663-5-43

Automatic Intrinsics and Extrinsics Projector Calibration with Embedded Light Sensors

Thomas Pönitz[1], Christoph Heindl[1], Andreas Pichler[1], Martin Kampel[2]

***Abstract*— We propose a novel projector calibration method based on embedded light sensors. Our method can be used to determine intrinsics and extrinsics of one or multiple projectors without relying on an additional camera. We show that our method is highly accurate and more than 17 times faster than state of the art methods. This renders our method suitable for spatial augmented reality applications in the industrial domain.**

I. INTRODUCTION

Augmented reality has become an important topic for industrial assembly. Workers are provided with localized and contextualized information to support them during difficult tasks. However in industrial environments special conditions prevail. Heat, dirt, gloves etc. impede the use of touch-screens. Wearables become cumbersome during long working hours and battery life is a constant concern.

As a solution to these problems spatial augmented reality (SAR) has gained traction. In SAR there are no monitors, head-mounted displays or hand-held devices. Instead physical objects become the canvas themselves. Information is either projected directly on the object of interest or objects next to it, e.g. a table surface, are used as screens. SAR does not obstruct workers in any kind Obstruction can be solved with multiple projectors targeting the same workstation.

In industrial settings high spatial precision is of special importance for SAR setups, therefore it is critical to achieve a highly accurate calibration of the SAR system's projectors.

II. STATE OF THE ART

To describe the intrinsics of a projector the same parameters as for cameras are used – focal lengths f_x, f_y, principal point (c_x, c_y) and radial and tangential distortion parameters k_i, p_j [1]. Determined by their intended use projectors exhibit very low distortion and it is typically sufficient to consider only k_1 and k_2.

In [3] a printed chessboard is observed by an uncalibrated camera. The projector projects a graycode based pattern as a series of images. The camera captures each of these projections. From these captured images it is possible to generate a homography mapping from camera pixel coordinates to projector pixel coordinates. Because both the camera and the projector exhibit distortions, a local homography is calculated around each chessboard corner. The camera pixel coordinates of all chessboard corners are determined with subpixel accuracy and mapped into projector pixel coordinates by the local homographies. At this stage the projector can be calibrated with standard methods for camera calibration, e.g. [4]. The drawback with this method is that an additional device, the camera, is needed. Projector and camera need to be synchronized which limits acquisition speed. The chessboard corner detection introduces additional complexity, processing time and error sources. The resolution of the pattern is limited by the camera as it has to resolve the fine pattern details.

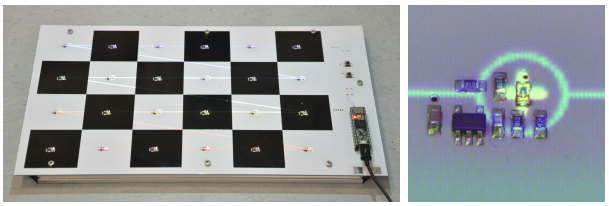

Fig. 1: Active calibration object with projected detections and detailed picture of the embedded light sensor.

[5] proposes a virtual pattern consisting of white and black circles. The black circles are printed as a physical pattern. The white circles are rendered in 3d using the projector's extrinsics and intrinsics and projected. A calibrated camera depicts the projected white circles and printed black circles onto an undistorted image. The centers of all circles are detected with subpixel accuracy.

The extrinsic and intrinsic parameters of the projector are iteratively adapted until black circle centers and white circle centers match exactly the virtual pattern. Similar drawbacks as described above apply. Additionally the camera needs to be calibrated beforehand and a starting solution has to be provided.

III. METHOD

To overcome the disadvantages of state of the art methods described in section II we propose a method without an additional camera.

Our method is based on [2], where embedded light sensors are placed on the corners of rectangular surfaces. We use sensors that have a radiant sensitive area of 0.23 square millimeter to observe a projected graycode pattern as in [5]. From the observed pattern the projector pixel coordinates can be determined and a homography is calculated. This allows to project onto the rectangle and let it act as a display. Furthermore a three dimensional object is equipped with sensors and the projector to object pose estimated, which enables projecting a texture onto the object.

However no intrinsics model is calculated, which is necessary for industrial high precision SAR, because even small distortions interfere with high-precision projections

[1]Profactor GmbH, 4407 Steyr-Gleink, Austria
[2]TU Wien, 1040 Vienna, Austria

and the intrinsics of Ultra Short Throw (UST) projectors can not simply be inferred from the projectors field of view specification. Therefore we propose the **active calibration object**, a three dimensional object equipped with embedded light sensors at well defined positions. Figure 1 depicts an early flat, rectangular prototype.

The hardware is capable of capturing 60 frames per second, as is currently the standard for projectors. For WUXGA resolution (1920 × 1200 pixel) the theoretical number of patterns is $\lceil \log_2(1920) \rceil + \lceil \log_2(1200) \rceil = 22$. To increase robustness against external lighting and resolve cases where pixel edges fall directly onto the sensors, we project each image followed by its inversion. Additionally we add two images at start and end which allows us to detect the beginning and ending of the pattern solely from the observed data. This results in a pattern length of $2+22\cdot 2+2=48$ and a total acquisition time of $\frac{48}{60}=0.8$ seconds, limited currently only by the frames per second of the projector.

In comparison [5] would need 46 pattern images for the same resolution (a white and black frame to gauge brightness levels instead of the two start and stop pattern images). Considering the time needed for the camera to acquire the image and projector latency, an optimistic estimate is 0.3 seconds per image, resulting in 13.8 seconds, which is $\frac{13.8}{0.8} = 17.25$ times slower.

IV. EXPERIMENTS

To evaluate our method we used two setups. First, our calibration object is mounted on a linear axis, with movement orthogonal to the object's plane and second, mounted on a wrist joint with two rotational axis, see figure 2. In the

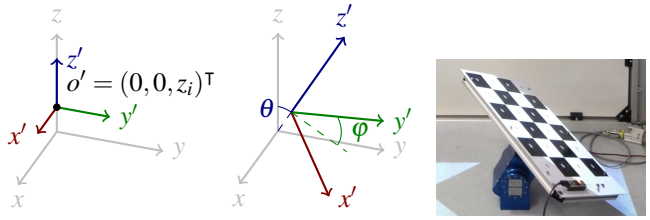

(a) (b) (c)

Fig. 2: Experimental setups: (a) variable height z_i and (b) wrist joint with two radial axis (θ rotates around x, φ around z'), illustrated in (c).

first setup we move the calibration object to 20 positions, equally spaced 1 cm apart, and acquire measurements, see figure 2a. We calibrate with these measurements stacked together, resulting in 12 degrees of freedom (6 extrinsics, 6 intrinsics f_x, f_y, c_x, c_y, k_1, k_2). Table I compares results of 15 calibrations from distinct measurements. In the second setup we rotate the calibration object around two axis, see figure 2b. θ assumes values $-35°,-30°,\ldots,35°$ and φ values $-135°,-130°,\ldots,45°$ – resulting in 555 positions total. Utilizing the projector intrinsics obtained from the prior setup we solve the PNP problem for each position resulting in calibration object poses and therefore a position $\mathbf{s}_{ijk} \in \mathbb{R}^3$ for every embedded light sensor (i$^{\text{th}}$ sensor, j$^{\text{th}}$ angle θ and k$^{\text{th}}$ angle φ). For each pose we compare the observed φ against the reported angle of the wrist joint, see table II.

Additionally for each angle $\theta_{j^\star}$ we fit a plane $P_{j^\star}$ through all sensor positions $\mathbf{s}_{ij^\star k}$. The distance of sensor position $\mathbf{s}_{ij^\star k}$ to plane $P_{j^\star}$ is $z_{ij^\star k}$. Sensor positions are projected onto their respective plane. When φ is varied, all plane points rotate around the same center point and all points belonging to the same sensor lie on the same circle. We obtain the center point and all circles, respectively their radii, by minimizing the square of the circle-point distances. The deviation of a point from its circle is $\mathbf{c}_{ij^\star k} = (x_{ij^\star k}, y_{ij^\star k})^\intercal$. We now form error vectors $\mathbf{e}_{ij^\star k} = (x_{ij^\star k}, y_{ij^\star k}, z_{ij^\star k})^\intercal$ and transform them into the projector coordinate system and compare them in table II as root mean square errors (RMSE) over angles θ_i.

Summarizing, we showed the high accuracy of our proposed system and its practicability for calibrating projectors in industrial SAR applications.

TABLE I: Mean and standard deviation over 15 calibrations of the root mean square reprojection-error (RMSE), focal lengths f_x, f_y, principal point $(c_x, c_y)^\intercal$ and radial distortion coefficients k_1, k_2. ($\alpha^\beta \triangleq \alpha \cdot 10^\beta$)

	RMSE	f_x	f_y	c_x	c_y	k_1	k_2
μ	7.6^{-1}	2,965.9	2,971.6	1,008	−76.7	-4.4^{-2}	6.6^{-2}
σ	1.9^{-2}	2.7	3.1	1.4	4	8.9^{-3}	2.7^{-2}

TABLE II: Root mean square error (RMSE) of angle φ and sensor positions $(x,y,z)^\intercal$ in projector coordinates, over angles θ. ($\alpha^\beta \triangleq \alpha \cdot 10^\beta$)

θ [°]	RMSE_φ [°]	RMSE_x [mm]	RMSE_y [mm]	RMSE_z [mm]
−35	2.8^{-2}	2.4^{-1}	1^{-1}	3.2^{-1}
−30	2.4^{-2}	2.2^{-1}	9.4^{-2}	3.4^{-1}
−25	2.4^{-2}	1.9^{-1}	6.6^{-2}	3.4^{-1}
−20	2.8^{-2}	1.5^{-1}	5.4^{-2}	3.7^{-1}
−15	2.3^{-2}	1.2^{-1}	5.6^{-2}	3.9^{-1}
−10	2^{-2}	6.2^{-2}	3.1^{-2}	3.1^{-1}
−5	1.9^{-2}	3.3^{-2}	2.1^{-2}	2.8^{-1}
0	1.7^{-2}	2.5^{-2}	2.3^{-2}	3.7^{-1}
5	1.9^{-2}	4.2^{-2}	3.2^{-2}	3.6^{-1}
10	2.3^{-2}	6.7^{-2}	5^{-2}	3.2^{-1}
15	2.3^{-2}	1.1^{-1}	6.6^{-2}	3.3^{-1}
20	2.3^{-2}	1.4^{-1}	7.5^{-2}	3.1^{-1}
25	2.5^{-2}	2.2^{-1}	1.2^{-1}	3.9^{-1}
30	3^{-2}	2^{-1}	1^{-1}	3.1^{-1}
35	2.7^{-2}	2.7^{-1}	1.5^{-1}	3.5^{-1}

REFERENCES

[1] R. Hartley and A. Zisserman, *Multiple View Geometry in Computer Vision*, 2nd ed. Cambridge University Press, 2003.

[2] J. C. Lee, P. H. Dietz, D. Maynes-Aminzade, R. Raskar, and S. E. Hudson, "Automatic projector calibration with embedded light sensors," in *Proceedings of the Symposium on User Interface Software and Technology*. ACM, 2004, pp. 123–126.

[3] D. Moreno and G. Taubin, "Simple, accurate, and robust projector-camera calibration," in *International Conference on 3D Imaging, Modeling, Processing, Visualization and Transmission*. IEEE, 2012, pp. 464–471.

[4] R. Y. Tsai, "An efficient and accurate camera calibration technique for 3d machine vision," 01 1986.

[5] L. Yang, J.-M. Normand, and G. Moreau, "Practical and precise projector-camera calibration," in *International Symposium on Mixed and Augmented Reality*. IEEE, 2016, pp. 63–70.

Acknowledgments The project leading to this application has received funding from the Fuel Cells and Hydrogen 2 Joint Undertaking under grant agreement No 735367. This Joint Undertaking receives support from the European Union's Horizon 2020 research and innovation programme and Hydrogen Europe and N.ERGHY.